The spatial, temporal, and amplitude characteristics of parallel electric fields associated with sub-solar magnetic field reconnection.

by F.S. Mozer[1] and P.L. Pritchett[2]

1. Space Sciences Laboratory, University of California, Berkeley, CA 94720
2. Department of Physics and Astronomy, UCLA, Los Angeles, CA 90095-1547

ABSTRACT

The three-component electric field experiment on the Polar satellite collected bursts of data at rates of 1600 and 8000 samples/second. Because data at rates at least as high as these are required for full resolution measurements of parallel electric fields associated with sub-solar magnetic field reconnection, some 150 such bursts from 2000 through 2003 were examined during five month intervals when the spacecraft was on the dayside of the Earth and the apogee of 9.5 R_E was near the equator. Seventeen events were found at or in the magnetopause having perpendicular electric fields as large as 200 mV/m and parallel electric fields as large as 80 mV/m. Fields of these magnitudes exceed those expected from simulations by an order-of-magnitude. The parallel electric fields were associated with plasma density depletions of more than a factor of two and they all appeared on the magnetospheric side of the current sheet. Their directions were such as to accelerate electrons that moved along the magnetic field towards the reconnection site. The full-widths-at-half-maximum of the parallel field events ranged from less than 0.2 to 15 milliseconds, in general agreement with results expected from simulation. Although the events occurred over ±20 degrees of magnetic latitude and for clock angles of 100 to 180 degrees, their statistics suggest that the X-line for these events was within a few degrees of the magnetic equator.

The Polar Satellite is the only space mission that has had the capability for measuring all three components of the electric field with mV/m sensitivity and thereby, to observe directly the parallel electric field associated with magnetic field reconnection at the dayside magnetopause. (Because the Polar apogee is ~9.5 Earth radii, it did not reach altitudes required for observing reconnection in the magnetospheric tail.) The statistical properties of >100 Polar satellite parallel electric field events have been published [*Mozer*, 2005]. These events came from data collected at 40 samples/second, so the time resolution was restricted to >25 milliseconds. At higher sampling rates, during occasional bursts of data at 1600 or 8000 samples/second, the typical durations of parallel electric field events at the magnetopause were much less than 25 milliseconds and the typical amplitudes of the fields were factors of 2-20 greater than measured at the lower resolution [*Mozer et al*, 2004]. These facts suggest the importance of obtaining statistics on parallel electric fields in burst events occurring at the sub-solar magnetopause. Toward this end, the bursts collected during January through May of 2000 through 2003, at radial distances greater than six Earth radii, were studied. These years and months were selected because the Polar apogee was on the dayside near the equator at these times. About 150 such bursts, having typical durations of ~25 seconds each, were found. Twenty seven of these bursts contained good examples of parallel electric fields and 26 others contained probable parallel electric fields that were not further analyzed. Of these

27 events, ten were rejected because they were not at or in the magnetopause. This left 17 high data rate events to be analyzed further. These analyses are the topic of this paper.

An example of three seconds of data from one such event is given in Fig. 1 in order to illustrate the difference between data collected at 40 and 1600 samples/second. The coordinate system for this and all data, other than that specifically labeled otherwise, is magnetic-field-aligned with the Z-axis parallel to the magnetic field, **B,** while the X-axis is perpendicular to **B** in the plane containing the magnetic field line and it is positive inwards. The Y-axis defines the third component of this right hand coordinate system by being perpendicular to **B** and pointing generally in the westward direction. Fig. 1 contains four pairs of panels that give the plasma density and the three components of the electric field at two different data rates. Panels a) and b) give the plasma density obtained from the spacecraft potential at rates of 1600 and 2.5 samples/second. Density fluctuations of more than a factor of two on short time scales in the high rate data of panel a) (which will be discussed) are completely missed at 2.5 samples/second in panel b). Similarly the nearly 200 mV/m E_Y electric field in panel e) and the parallel electric field >50 mV/m in panel g), are underestimated in the data at 40 samples/second by factors greater than 10.

Measurement of a parallel electric field may be uncertain because:

- it may be as small as 10% of the perpendicular electric field, so geometric misalignments can produce apparent parallel electric fields,
- the magnetic field is not measured with the time resolution of the electric field, so the B-field is linearly interpolated to the times of E-field measurements. If the rapidly changing magnetic field does not vary linearly, apparent parallel electric fields can result,
- the short, spin-axis electric field measurement [*Harvey et al*, 1995] is uncertain due to its proximity to perturbations from the spacecraft. This may introduce significant noise in the parallel field estimate, depending on the geometry of the situation.
- Solitary waves and other wave modes produce valid parallel electric fields that must be distinguished from the parallel electric fields directly associated with magnetic field reconnection because such wave fields are not of interest to the present studies.

Because the Polar spacecraft was in a cartwheel mode, one of the pair of on-axis sensors was shadowed by the spacecraft in the vicinity of the dawn-dusk orbit, and the resulting on-axis data is not usable. However, in the noon-midnight orbit, there is a high level of symmetry between these sensors, the spacecraft, its photoemission, and the sun. This causes any perturbation from photoemission, for example, to be the "same" on the two axial sensors, so this perturbation cancels when the potential difference is measured. However, one of the on-axis sensors is closer than the other to the center of the 1/r potential from the charged spacecraft because the despun platform extends on one side of the spacecraft to spoil the axial symmetry. For this reason, it is necessary to subtract ~200 millivolts from the measured potential difference along the spin axis to obtain a field that is small in regions where the spin-plane-measured fields are small. Other than

adjusting this offset, there are no special corrections made to the on-axis measurements. A discussion of the methods for validating a parallel electric field measurement is given in Appendix A.

Electric and magnetic fields associated with a magnetopause crossing at a geocentric distance of 9.1 Earth radii, a magnetic local time of 1100, and a magnetic latitude of 10.3 degrees are given in GSE coordinates in Fig. 2. That the spacecraft traveled from the magnetosphere to the magnetosheath during this 15 second interval is evidenced by the panel a) increase of plasma density from about 1 to 4 particles/cm^3 and by the GSE Z-component of the magnetic field changing in panel d) from the magnetospheric value of 90 nT to about -25 nT in the magnetosheath. The largest electric fields in panels e), f), and g) occur at the magnetospheric side of the current sheet, as discussed earlier for asymmetric reconnection [*Mozer et al*, 2008] and as will be important when considering the spatial distribution of large parallel electric fields. The three second interval between the two vertical lines in Fig. 2 is expanded in Fig. 1 as burst electric field data in the field aligned coordinate system. The 0.5 second interval between the vertical lines in Fig. 1 is expanded and displayed in Fig. 3. Again it is noted that the low data rate data of panels b), d), f) and h) in Fig. 3 underestimate the associated burst amplitudes of panels a), c), e), and g) by factors of more than two for the density fluctuations of panel a) and more than 10 for the electric field components.

The parallel electric field of panel g) in Fig. 3 contains contributions of three kinds. Between 0.4 and 0.5 seconds, large amplitude wave fields are present. Throughout the plot but especially between 0.22 and 0.25 seconds, bipolar solitary waves are observed. While important, neither of these types of field matter for the present discussion. What is important in this panel are the positive parallel electric fields seen at the locations of the six vertical lines in the figure. They have typical amplitudes of 10-40 mV/m and durations of ~8 msec. With one exception, they are not observed at the low data rate. Although there are at least six parallel electric field examples in this figure, for purposes of the statistics discussed below, they are treated as a single parallel electric field event.

The vertical lines from the parallel electric field events in Fig. 3 show that they occurred in the presence of perpendicular electric fields of up to 200 mV/m in panels c) and e) and in plasma depletions greater than a factor of two in panel a). Magnetic field fluctuations measured by the search coil magnetometer (not shown) are uncorrelated with the parallel electric fields and have magnitudes of a few tenths of a nanoTesla. Because the ratio of the electric to magnetic field is greater than the velocity of light, these parallel electric field structures must be electrostatic.

The locations and properties of the 17 events analyzed in this study are given in Table 1. As seen from the relative strength of the reconnection magnetic field, B_Z, in column I, all of the events occurred on the magnetospheric side of the current layer. This result may be compared to simulations of the parallel electric field in Fig. 4 [*Pritchett*, 2008], in which, everywhere other than near the reconnection site at the center of the figure, the largest parallel electric fields occur on magnetospheric field lines. Because it is not expected that the spacecraft would be near the reconnection site frequently, the fact that

all the events in the data set occurred on magnetospheric field lines is in agreement with simulations.

Both the simulation of Fig. 4 and analyses of electron data (Egedal et al, 2009 and references therein) require that the parallel electric field away from the reconnection site have the sense appropriate to accelerate electrons moving along the field line towards the reconnection site. That is, the parallel electric field should be upward above the X-line and downward below it. This prediction may be tested on the 17 events by using the sign of $(\mathbf{E}x\mathbf{B}/B^2)_Z$ in GSE coordinates to determine whether the observation was north or south of the reconnection site. If an event occurred north of the reconnection site and on the magnetospheric side of the current sheet, the signs of $(\mathbf{E}x\mathbf{B}/B^2)_Z$ and B_Z, in GSE, would be positive, as should the sign of the parallel electric field if it has the sense to accelerate incoming electrons. Similarly, for parallel electric fields of the expected sign either above or below the reconnection site and either on magnetospheric or magnetosheath magnetic field lines, the product of the three signs should be positive. The signs of $(\mathbf{E}x\mathbf{B}/B^2)_Z$, B_Z and the parallel electric field are given for each of the 17 events in columns F, G, and H, of Table 1. It is seen that 15 of the 17 events satisfy the criteria expected if the parallel electric field had the direction to accelerate incoming electrons towards the reconnection site. This result would happen by chance with a probability less than 0.001 if the parallel electric fields had random directions. This result is a strong verification of both the quality of the parallel electric field measurement and the validity of the theory and simulation.

The amplitudes of the observed parallel electric fields, given in column K of Table 1, varied from 5 to 82 mV/m. The simulation fields of Fig. 4, when converted from normalized to physical units, have magnitudes <8 mV/m. This order-of-magnitude discrepancy between simulation and space data is not understood.

Column L of Table 1 gives the full-width-at-half-maximum of the durations of the events, which varied from 1 to 14 milliseconds. In addition, 10 one point events at 1600 samples/second and 4 one point events at 8000 samples/second were observed and not counted because they did not yield valid estimates of the amplitude or duration. This result suggests that fully capturing rapid parallel electric field events requires sampling the data at >20,000 Hz.

The time scales of the observed and simulation events may be compared via the movie of simulation parallel electric fields given in the accompanying movie. This movie covers a spatial region of 1.5 ion skin depths by 2.0 ion skin depths. The parallel electric field structures have sizes the order of one or a few electron skin depths. Because the mass ratio of the simulation was 200, the duration of the movie depends on whether the ions are light or the electrons are heavy. Because parallel electric fields are associated with electron physics, it is assumed that the ions are light, in which case, the duration of the movie is 0.3 seconds. Fig. 5 gives the power spectrum of the electric field fluctuations observed at a point in the simulation space. The power peaks around the electron cyclotron frequency, which is 1500-2500 Hz in the space data. This time scale is

in general agreement with the durations observed in Table 1 if the parallel electric fields in space occur in groups, as they do in Figs. 3 and A1.

Panel b) of Fig. 6 presents the clock angle of each event (angle between the magnetic field vector in the magnetosphere and the magnetic field vector in the magnetosheath) as a function of the magnetic latitude of the observation. The two small clock angles in this panel should be ignored because they are associated with partial crossings of the current sheet during which the full magnetosheath magnetic field was not observed. Panel a) of Fig. 6 presents the sign of $(\mathbf{E}x\mathbf{B}/B^2)_Z$ as a function of magnetic latitude. The sign is interpreted as describing whether the event of interest occurred north or south of the reconnection site, as discussed earlier. The signs are not distributed randomly because all northern magnetic latitude events were also north of the reconnection site and most of the southern latitude events were south of the reconnection site. The probability of this result occurring by chance if the sign of $(\mathbf{E}x\mathbf{B}/B^2)_Z$ was random is 0.006. Thus, these data suggest that, for clock angles greater than about 100 degrees, the reconnection site is within a few degrees of the magnetic equator. This result is different from a common cartoon so it will be further studied in a later publication.

In summary, the three-component electric field experiment on the Polar satellite collected bursts of data at rates of 1600 and 8000 samples/second. Because data at such rates and higher is required for full resolution measurements of parallel electric fields associated with sub-solar magnetic field reconnection, some 150 such bursts, occurring from 2000 through 2003 during five month intervals when the spacecraft was on the dayside of the Earth and the apogee of 9.5 R_E was near the equator, were found and analyzed. Of the more than 50 events containing parallel electric fields, 17 that occurred at or in the magnetopause were selected for further analysis before it was known where they occurred. These events had perpendicular electric fields as large as 200 mV/m and parallel electric fields as large as 80 mV/m. Fields of these magnitudes exceed those expected from simulations by an order-of-magnitude. The parallel electric fields were associated with plasma density depletions of more than a factor of two and they all appeared on the magnetospheric side of the current sheet. Because the magnetic field fluctuations were less than a nanoTesla, these structures were electrostatic. Their directions were such as to accelerate electrons that moved along the magnetic field towards the reconnection site. The full-widths-at-half-maximum of the parallel field events ranged from less than 0.2 to 15 milliseconds, in general agreement with results expected from simulation. Although the events occurred over ±20 degrees of magnetic latitude and for clock angles of 100 to 180 degrees, the statistics suggest that the X-line for these events was within a few degrees of the magnetic equator.

One may qualitatively estimate the electric potential associated with these parallel fields to determine if it is consistent with the 15 kV potential required by analyses of electron data in the tail [*Egedal et al,* 2009]. For this purpose, the parallel potential is estimated as the product ZEf, where Z is the distance along the field line that the potential exists, E is the average electric field, and f is the fraction of the field line that contains this average electric field. If $f \approx 0.01$, and $E \approx 50$ mV/m, the Z distance over which the potential is 15 kV is $\sim 5R_E$. The largest magnetic latitude at which such fields were

observed on Polar corresponded to a distance from the reconnection site of $3R_E$. Higher latitude observations were not possible because the 9.5 R_E apogee of the satellite diminished the number of magnetopause crossings at higher latitudes. Thus, direct observations of parallel electric fields are consistent with the possibility of a 15 kilovolt potential along the magnetic field line over reasonable distances because such fields are an order-of-magnitude larger than predicted from simulations,.

APPENDIX A. Validating a parallel electric field measurement

The techniques for validating a parallel electric field measurement have been discussed (Mozer, 2005). A further example of these techniques is given in Fig. A1. In this figure, the electric field components in the magnetic-field-aligned coordinate system are obtained in three ways:

- from the measured three components of the electric field
- by discarding the on-axis measurement and assuming, in its place, that the component along the spacecraft spin axis, V56, is zero.
- by discarding the on-axis measurement and assuming, in its place, that the parallel electric field is zero

Panels a), b), and c) of Fig. A1 give the X-component of the electric field computed in the three ways, panels d), e), and f) give the Y-component, and panels g) and h) give the Z-component (the Z-component computed under the assumption that $\mathbf{E}\cdot\mathbf{B} = 0$ is not given because it is zero). The figure presents one second of data at a geocentric distance of 9.18 Earth radii, magnetic local time of 1450, and magnetic latitude of -8.9 degrees. Note that the scales of the electric field plots differ for the different field components. The values of E_X computed by the three methods in panels a), b) and c) are essentially identical because the X-direction happened to be perpendicular to the spacecraft spin axis for this and many crossings because they occurred near local noon with the spin axis in the east-west direction.. The value of E_Y computed by assuming that the on-axis field was zero (panel e)) is small because the Y-direction was nearly parallel to the spin axis.

Consider the data during the first 0.25 seconds of Fig. A1, during which there is strong evidence that the parallel electric field was zero and that the short, on-axis field measurement worked well. This evidence comes from the facts that:

1. the three-component measurement of the parallel electric field in panel g) was generally zero (with one exception that was probably a non-zero parallel field). Note that the parallel field was zero because the non-zero parallel field of panel h), obtained by assuming that the on-axis field was zero, was canceled by the actual measurement of this third component. This shows that the short axial electric field boom on Polar functioned properly.
2. The three-component measurement of E_Y in panel d) agrees well with the panel f) two component measurement and the assumption that the parallel field was zero.

Now, consider the measurements during the final 0.4 seconds of the figure.

1. The data in panels g) and h) generally agree, which means both that the parallel electric field was non-zero and that the parallel measurement was made primarily by the more reliable spin-plane wire booms.
2. Panels d) and f) differ greatly. This is because, in the presence of a non-zero parallel electric field, the E_Y required to force the parallel component to be zero in panel f) was huge.

The verified parallel electric field measurements in panel g) include bipolar solitary waves at times such as 0.68, 0.72, 0.92, and 0.95 seconds and relatively large, unipolar parallel electric fields of the type searched for in this paper at times such as 0.76, 0.80, and 0.86 seconds. Although there are at least three such events in this time interval, it is reported as a single event in the statistics of Table 1.

ACKNOWLDEGEMENTS

This research was supported by NASA grants NNX08AM15G, NNG05GL27G, and NNG05GC72G and Contract NAS5-02099-07/09. The particle simulations were performed using resources of the San Diego Supercomputer Center (supported by the National Science Foundation under cooperative agreement ACI-9619020) and the UCLA Dawson Cluster (funded by NSF grant PHY-0321345).

FIGURE CAPTIONS

Figure 1. Three seconds of plasma density and electric field data obtained on the Polar satellite at two data rates.

Figure 2. Plasma density and electric and magnetic fields measured in GSE coordinates during a 15 second crossing of the sub-solar magnetopause.

Figure 3. 0.5 seconds of plasma density and electric field data obtained at two data rates during a sub-interval of the times illustrated in Figs. 1 and 2.

Figure 4. Parallel electric fields determined by an open, driven, asymmetric simulation with a mass ratio of 200. The color scale is saturated such that the blue and red colors include all data within a factor of three of the peak value.

Figure 5. Power spectrum of the parallel electric field fluctuations measured in a simulation of magnetic field reconnection.

Figure 6. The clock angle and the sign of $(\mathbf{E}x\mathbf{B}/B^2)_Z$ measured as functions of magnetic latitude during 17 parallel electric field events at magnetopause crossings.

Figure A1. Electric fields determined three different ways during and before a parallel electric field event.

REFERENCES

Egedal, J., A. Le, N. Katz, L.-J. Chen, B. Lefebvre, and W. Daughton (2009), Cluster observations of bi-directional beams caused by electron trapping during anti-parallel reconnection, J. Geophys. Res., submitted

Harvey, P., et al. (1995), The electric field instrument on the Polar satellite, Space Sci. Rev., 79, 583.

Mozer, F. S., S. D. Bale, J. D. Scudder (2004), Large amplitude, extremely rapid, predominantly perpendicular electric field structures at the magnetopause, Geophys. Res. Lett., 31, L15802.

Mozer, F. S. (2005), Criteria for and statistics of electron diffusion regions associated with sub-solar magnetic field reconnection, J. Geophys. Res., 110, A12222, doi:10.1029/2005JA011258.

Mozer, F. S., P. L. Pritchett, J. Bonnell, D. Sundkvist, and M. T. Chang (2008), Observations and simulations of asymmetric magnetic field reconnection, , J. Geophys. Res., 113, A00C03.

Pritchett, P. L. (2008), Collisionless magnetic reconnection in an asymmetric current sheet, J. Geophys. Res., 113, A06210, doi:10.1029/2007JA012930.

.TABLE 1. SEVENTEEN PARALLEL ELECTRIC FIELD EVENTS

A	B	C	D	E	F	G	H	I	J	K	L	M
DATE	TIME	RE	MLT hours	MLAT degrees	(EXB)Z sign	BZ sign	Epar sign	BZ/Bmax	Eperp mV/m	Epar mV/m	FWHM msec	clock angle degrees
4/17/2000	01:47:45.4	9.21	11.1	24.46	1	1	1	0.93	67	5	12.0	172
5/17/2000	01:46:45.1	7.78	9.23	3.5	1	1	1	0.60	83	17	2.3	168
3/20/2001	01:23:32.2	9.26	12.3	9.5	1	1	-1	0.82	27	-20	1.0	129
4/1/2001	23:24:56.6	9.18	11.6	9.91	1	1	1	0.75	90	42	2.7	165
4/2/2001	00:20:58.8	9.41	11.6	12.08	1	1	1	0.80	60	65	1.2	143
4/13/2001	09:37:48.1	9.09	11	10.27	1	1	1	0.64	198	35	8.0	129
1/19/2002	16:20:11.4	8.04	15.7	-8.67	1	1	1	0.87	30	12	15.0	9
4/2/2002	04:51:18.2	8.97	11	-17.96	1	1	1	0.94	65	45	1.7	162
4/2/2002	04:51:18.3	8.97	11	-17.5	1	1	-1	0.94	140	-82	1.8	162
4/27/2002	11:48:52.6	9.58	9.49	11.56	1	1	1	0.83	50	14	6.0	22
5/10/2002	10:20:57.6	9.52	8.55	6.58	1	1	1	0.96	32	32	7.0	117
5/11/2002	22:25:34.9	9.42	8.91	-10.64	-1	1	-1	0.90	90	-10	5.0	139
1/24/2003	20:01:32.1	9.18	14.8	-8.93	-1	1	-1	0.67	25	-20	4.0	105
3/2/2003	11:38:32.1	9.3	12.3	-18.83	-1	1	-1	0.96	26	-13	4.0	126
3/31/2003	13:16:02.5	9.25	10.5	-12.72	-1	1	-1	0.40	72	-67	2.3	162
3/31/2003	13:16:03.0	9.25	10.5	-12.3	-1	1	-1	0.40	55	-35	1.6	162
4/4/2003	11:12:35.1	9.59	10.3	-7.45	-1	1	-1	0.87	40	-14	1.9	172

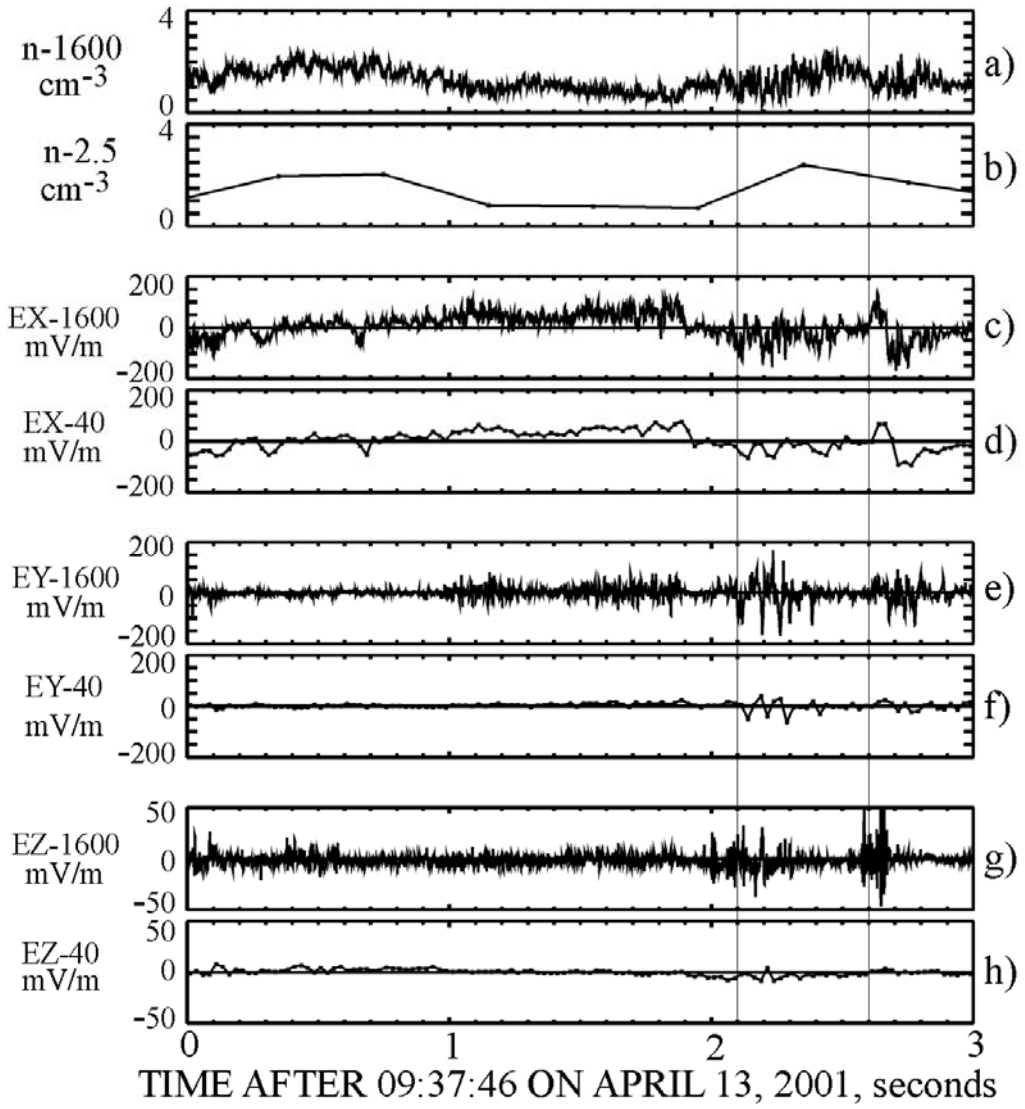
n-1600
cm-3
4
0
a)
n-2.5
cm-3
4
0
b)
EX-1600
mV/m
200
0
-200
c)
EX-40
mV/m
200
0
-200
d)
EY-1600
mV/m
200
0
-200
e)
EY-40
mV/m
200
0
-200
f)
EZ-1600
mV/m
50
0
-50
g)
EZ-40
mV/m
50
0
-50
h)
0
1
2
3
TIME AFTER 09:37:46 ON APRIL 13, 2001, seconds

FIGURE 1

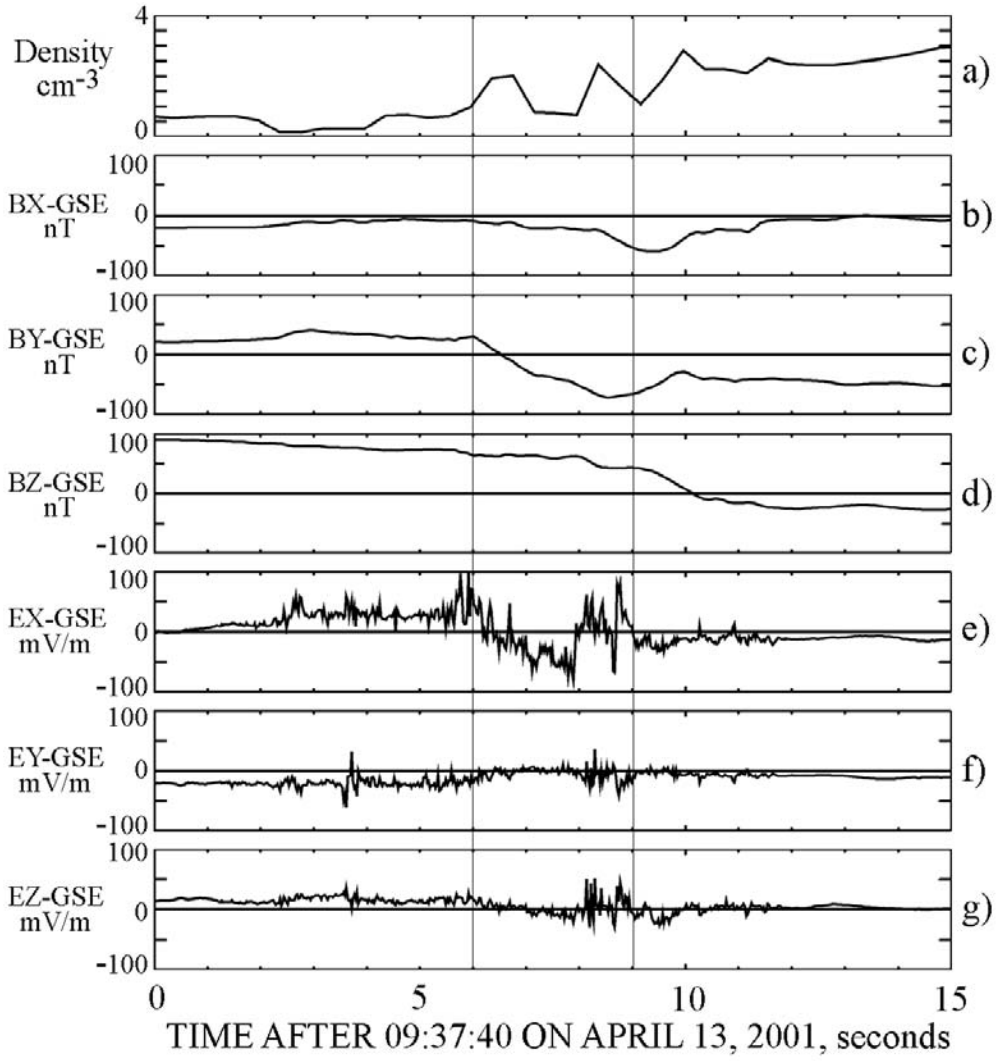
Density
cm-3
4
0
a)
BX-GSE
nT
100
0
-100
b)
BY-GSE
nT
100
0
-100
c)
BZ-GSE
nT
100
0
-100
d)
EX-GSE
mV/m
100
0
-100
e)
EY-GSE
mV/m
100
0
-100
f)
EZ-GSE
mV/m
100
0
-100
g)
0
5
10
15
TIME AFTER 09:37:40 ON APRIL 13, 2001, seconds

FIGURE 2

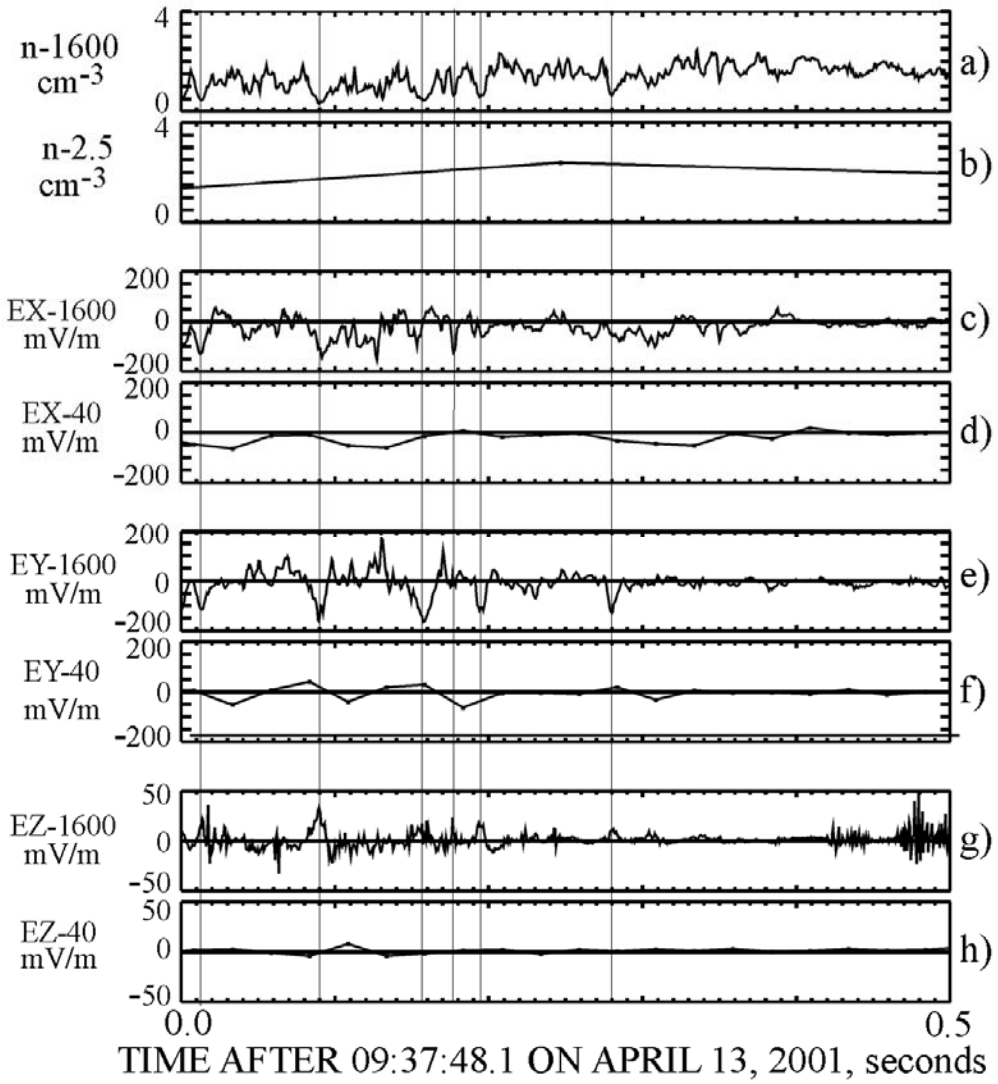
n-1600
cm-3
4
0
a)
n-2.5
cm-3
4
0
b)
EX-1600
mV/m
200
0
-200
c)
EX-40
mV/m
200
0
-200
d)
EY-1600
mV/m
200
0
-200
e)
EY-40
mV/m
200
0
-200
f)
EZ-1600
mV/m
50
0
-50
g)
EZ-40
mV/m
50
0
-50
h)
0.0
0.5
TIME AFTER 09:37:48.1 ON APRIL 13, 2001, seconds

FIGURE 3

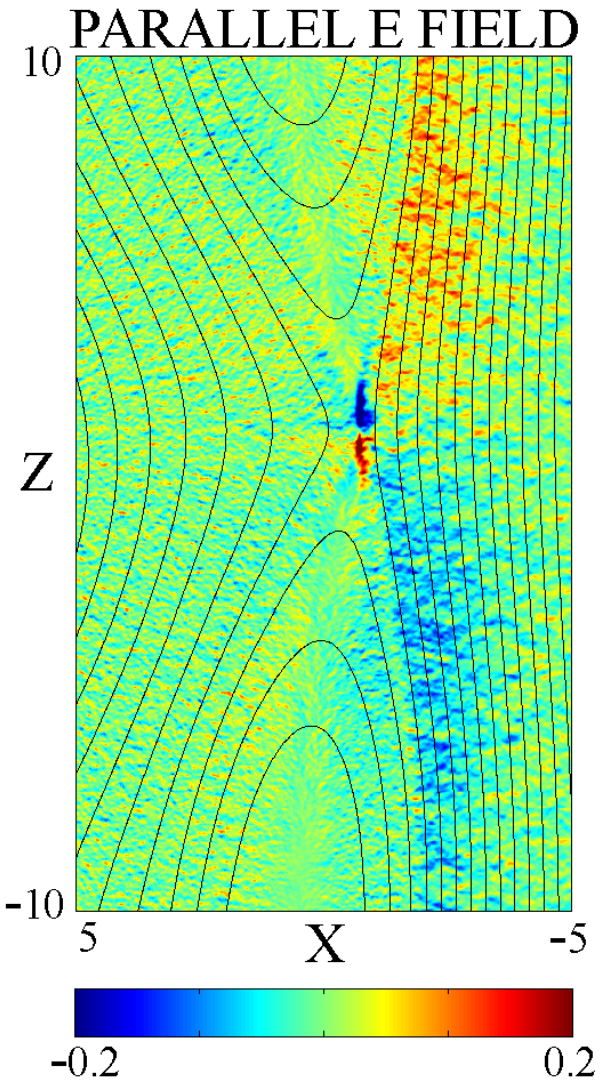

FIGURE 4

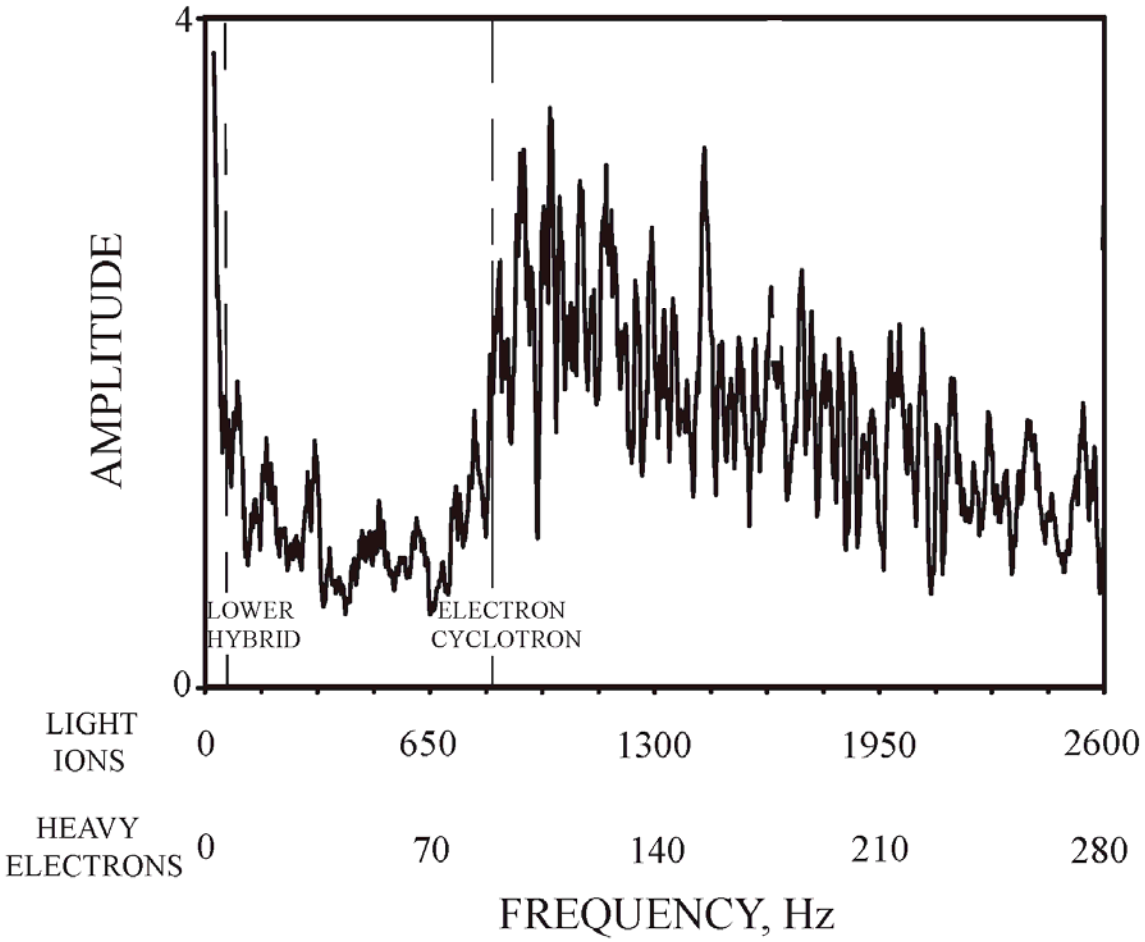
4
AMPLITUDE
0
LOWER
HYBRID
ELECTRON
CYCLOTRON
LIGHT
IONS
0
650
1300
1950
2600
HEAVY
ELECTRONS
0
70
140
210
280
FREQUENCY, Hz

FIGURE 5

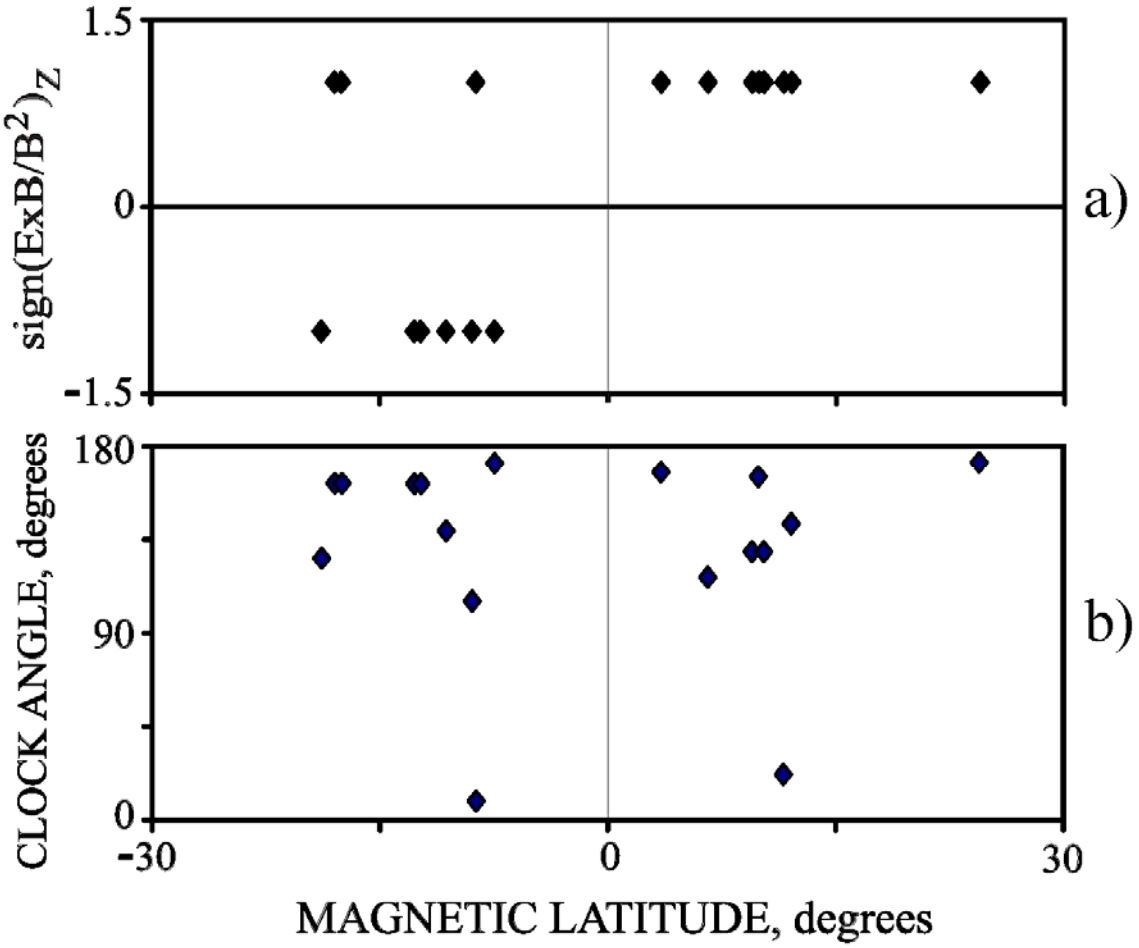
1.5
0
-1.5
sign(ExB/B2)Z
a)
180
90
0
CLOCK ANGLE, degrees
b)
-30
0
30
MAGNETIC LATITUDE, degrees

FIGURE 6

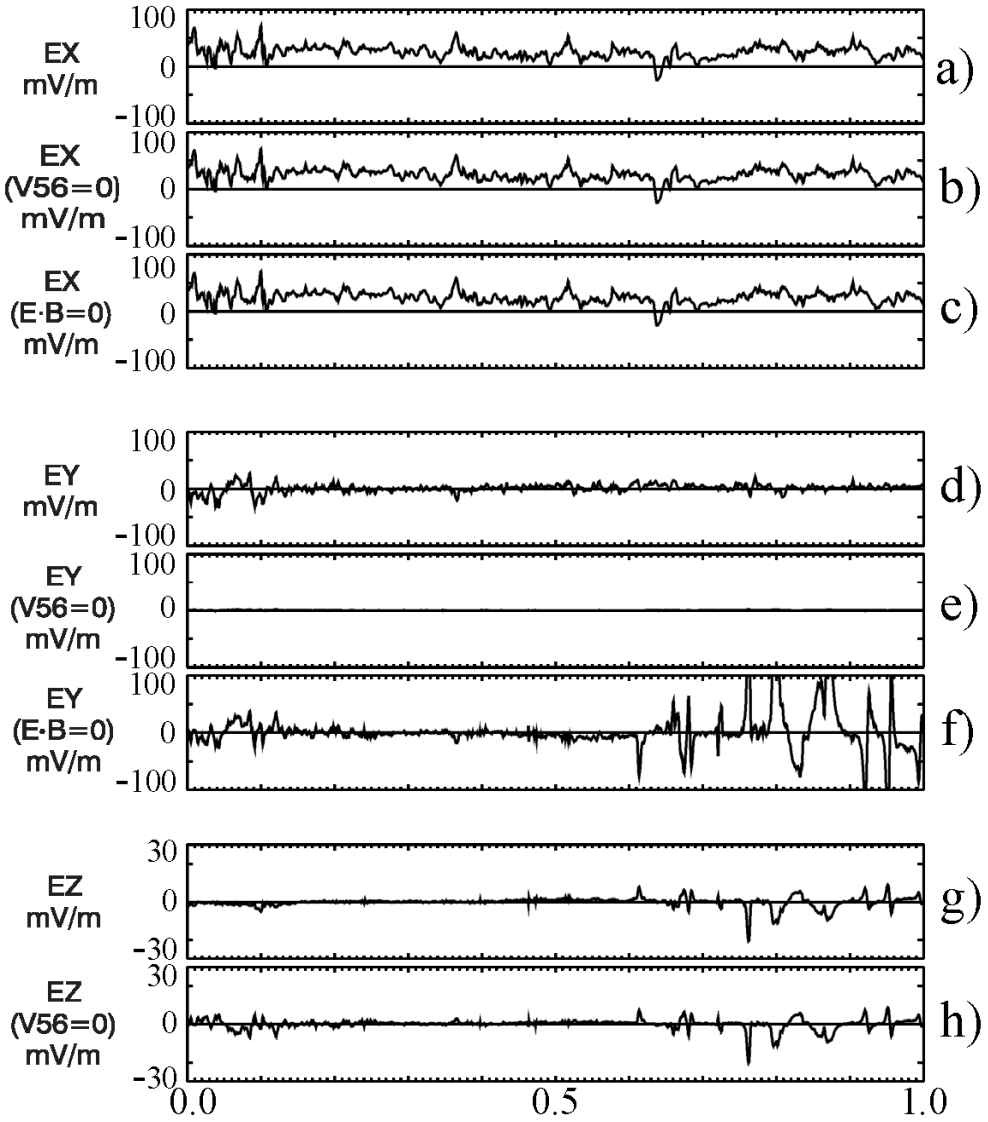
EX
mV/m
100
0
-100
a)
EX
(V56=0)
mV/m
b)
EX
(E·B=0)
mV/m
c)
EY
mV/m
d)
EY
(V56=0)
mV/m
e)
EY
(E·B=0)
mV/m
f)
EZ
mV/m
30
-30
g)
EZ
(V56=0)
mV/m
h)
0.0
0.5
1.0
TIME AFTER 20:01:31.4 ON JANUARY 24, 2003, seconds

FIGURE A1